UNIVERSITY OF ALBERTA

Morphometric Comparisons Between Rogen Terrain and Hummocky Terrain

By

David Olen Burgess ©

A thesis submitted to the Faculty of Graduate Studies and Research in partial fulfillment of the requirements for the degree of Master of Science.

DEPARTMENT OF GEOGRAPHY

Edmonton, Alberta
Spring 1994

ISBN 0-612-11167-9

UNIVERSITY OF ALBERTA

RELEASE FORM

NAME OF AUTHOR: **David Olen Burgess**

TITLE OF THESIS: **Morphometric Comparisons Between Rogen Terrain and Hummocky Terrain**

DEGREE: **Master of Science**

YEAR THIS DEGREE WAS GRANTED: **1994**

#201 10434-77ave
Edmonton, Alberta
T6E 1M8

January 27, 1994

UNIVERSITY OF ALBERTA

FACULTY OF GRADUATE STUDIES AND RESEARCH

The undersigned certify that they have read, and recommend to the Faculty of Graduate Studies and Research for acceptance, a thesis entitled **Morphometric Comparisions Between Rogen Terrain and Hummocky Terrain** submitted by **David Burgess** in partial fulfillment of the requirements for the degree of Master of Science.

J. Ronald Eyton
Professor Ron Eyton

J. Shaw
Professor John Shaw

Professor Arthur Peterson

December 22, 1993

University of Alberta

Inter-departmental Correspondence

to: Faculty of Graduate Studies

date: 24 January 1994

our file:

from: Dr. John Shaw
Department of Geography

your file:

subject: **Copyright**

I am pleased to give David Burgess permission to use a copy of Figures 14 and 16 from Glacial Facies Models in his thesis and any subsequent publications.

John Shaw

John Shaw
Professor and Chair

JS/fm

ABSTRACT

Visual interpretation of the aerial photographs suggests that certain geomorphological similarities exist between the hummocky terrain of central Alberta, Canada and the Rogen terrain of the Northwest Territories, Canada. This study statistically compares the two land form types based on measures of depressional form shapes and ridge orientations. Three sample areas (H1, H2, and H3) were selected from the hummocky terrain study site for comparision with one sample area (ROG) selected from the Rogen terrain study site. Sample areas H1 and H2 were chosen as representative areas of hummocky terrain that were similar in appearance to the Rogen terrain. Sample area H3 was selected because it contained the typically random pattern normally associated with hummocky terrain. Four different shape index values were calculated for the depressional form shapes comprising each sample area. Statistical comparision between sample areas based on shape index values indicated that sample areas H1, H2, and ROG were significantly similar and sample areas H3 and ROG were significantly dissimilar. Orientation analysis indicated that the ridges of sample areas H1, H2, and ROG all exhibited a preferred trend, while the ridge orientations of sample area H3 were uniform. Significant similarities between the hummocky terrain and the Rogen terrain based on the dominant properties common to each land form indicate that a similar two-dimensional pattern is evident in both land forms, hence, similar geomorphological processes may have been responsible for both terrain types. Variability in the formation process would explain why only particular areas throughout the hummocky terrain exhibit patterns similar to the Rogen terrain and others do not (such as sample area H3). Comparision of depressional form measures and ridge orientation analysis indicates that the hummocky terrain of central Alberta and the Rogen terrain of the Northwest Territories appear to have a common or similar origin.

ACKNOWLEDGMENTS

I would like to thank my supervisor, Dr. Ron Eyton, for his tremendous support and enthusiasm throughout this project. His straight forward approach to research made this a rewarding and valuable learning experience. I am indebted to Dr. John Shaw who helped initiate this project and provided valuable geomorphological insight along the way. The constructive critisism and keen interest shown by my external commitee member, Art Peterson, was also greatly appreciated. Thanks to Dan Hemmenway, whose computer related assistance was invaluable, Randy Pakan and Dave Epp, for the photographic services, and Geoff Lester for all cartographic work provided. I would like to acknowledge all the great people I met in Geography who made this a truly memorable experience. Finally, a special thanks to Caroline for all her love and support.

TABLE OF CONTENTS

LIST OF TABLES

LIST OF FIGURES

LIST OF PLATES

1. INTRODUCTION

Visual analysis of land form characteristics provides the basis for recognizing, examining, and comparing geomorphological patterns and form. However, interpretive comparisons between two land form types based on detailed or subtle properties may be not be widely accepted by others due to potentially biased views. In these cases, where subjective analysis is generally not accepted, comparison of form can be based on measurements. Quantitative comparisons between land forms reduce subjective interpretation and thus decreases the possibility of presenting biased results.

Morphometric analysis examines the measurable characteristics of land forms and provides a quantitative basis for geomorphological interpretations. See King (1974) for a review of these techniques applied to glacially formed landscapes. The latest major North American ice advance produced a wide variety of geomorphological features for interpretation. Two such features are Rogen terrain (Plate 1) and hummocky terrain (Plate 2). Rogen terrain has been compared in form to the erosional patterns found on the underside of river ice, suggesting that subglacial meltwater processes may have been responsible for the formation of this land form (Shaw, 1988; Fisher and Shaw, 1992). Although the 'ripple' pattern characteristic of Rogen terrain occurs only in particular locations throughout hummocky terrain, the overall intense undulating nature of hummocky terrain suggests that fluvial processes may have been an integral factor in the formation of this land form type as well. Morphometric comparisons between Rogen terrain and hummocky terrain are based on two dominant physical properties: shape of depressional forms, and ridge orientations. These properties are common to both land forms and should indicate whether or not the similarities are statistically significant. Depressions common to the Rogen terrain and the hummocky terrain are assumed to be the direct results of the mechanisms by

Plate 1. Rogen terrain with water-filled depressions in the North West Territories, Canada. North is to the top of photograph. Scale = 1:60,000. Source: National Air Photo Library.

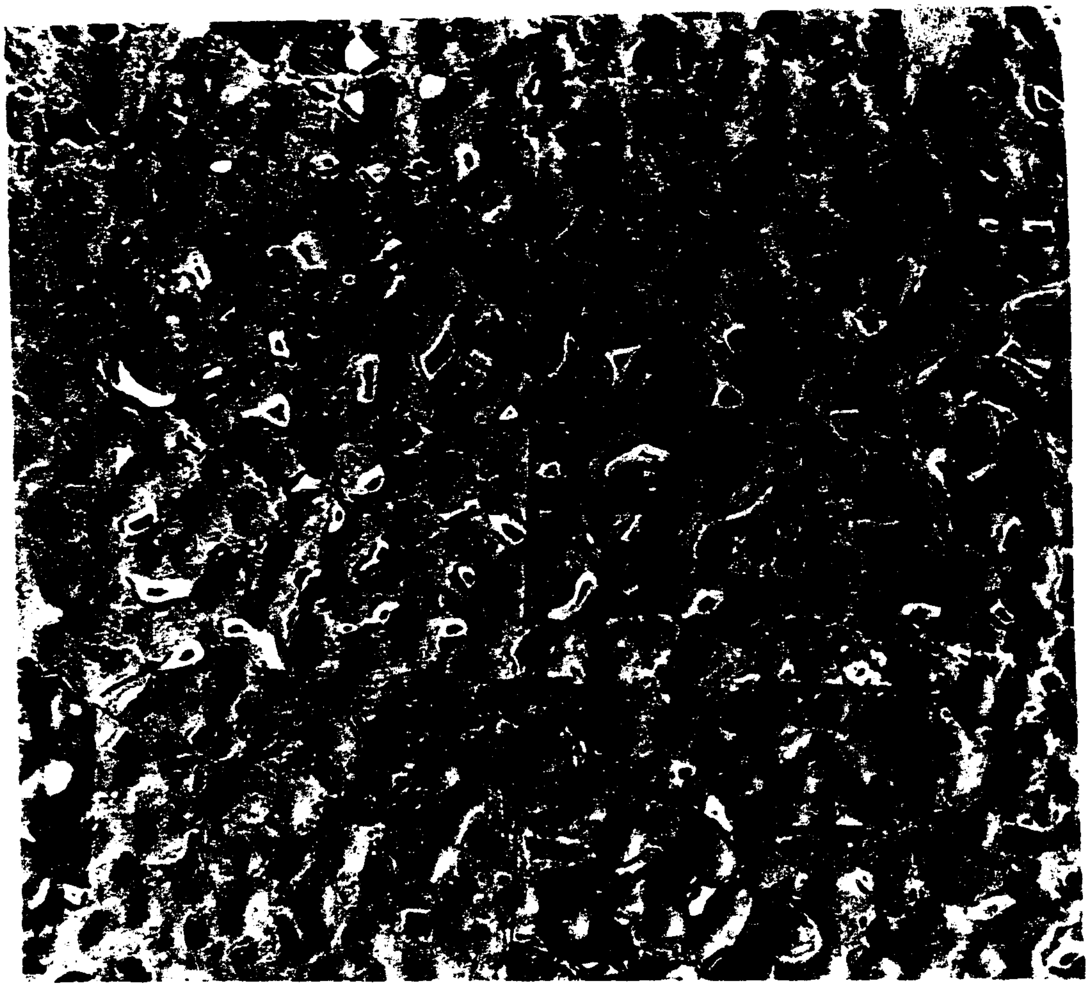

Plate 2. Hummocky terrain in central Alberta, Canada. North is to the top of photograph. Scale = 1:15,000.
Source: National Air Photo Library.

which both landscapes were formed. Modification of the depressions by human or natural erosion processes since the time of formation should not have altered the depressional form shapes significantly. Ridge orientations from each land form will also be analyzed and statistically tested for a preferred trend. If statistically significant similarities exist (based on depressional forms and ridge orientation analysis) between the hummocky terrain and the Rogen terrain, then this may suggest a similar formative process for both land forms.

The specific objective of this study is to apply analytical cartographic techniques to land form comparison. Depressional form shapes from the Rogen terrain and the hummocky terrain are measured and statistically compared. Ridge orientations from each land form are measured and tested for a preferred orientation. Statistically significant similarities between the two land forms support a similar genesis for the Rogen terrain of the Northwest Territories and the hummocky terrain of central Alberta.

2. BACKGROUND

Rogen Terrain

Although a variety of explanations have been put forward to explain the origin of Rogen terrain, most theories have invoked subglacial processes as the predominant mode of formation. Sugden and John (1977) postulated that a zone of compressive flow resulted as the glacier advanced over topographic concavities (Figure 1). Flow in these compressive zones decelerated and deformation of the ice mass created a series of transverse folds where debris accumulation occurred, eventually resulting in the formation of Rogen terrain ridges. Lundqvist (1969), on the other hand, suggested that Rogen terrain was formed in association with major transverse crevasses in the basal ice into which till was squeezed. Based on till fabric analysis, Cowan (1968) proposed that as the ice advanced, a build-up of material at the snout of the glacier would create a significant amount of resistance, forcing the glacier to over-ride this material. After the debris had been over-ridden, a subsequent accumulation of material would again occur and the process would be repeated forming a series of transverse ribs. Henderson (1959) examined the composition of Rogen moraine in the Dyke Lake area of Labrador, Canada, and concluded that the ridges were the result of annual accumulations of debris marking the terminus of the retreating ice sheet. Rogen moraine near Esker Lake, Labrador, Canada, was studied by Ives (1956) and found to be formed in close association with large trunk eskers in that area. Hydrostatic pressure from proglacial lakes (Hughes,1964, quoting from J.G. Fyles) was thought to play an integral part in the formation of Rogen terrain.

Recent interpretations based on form analogy provided evidence to suggest a subglacial meltwater origin for Rogen terrain (Fisher and Shaw, 1992). Figure 2 shows Rogen terrain in relation to other bed forms created by infilling of sediments into subglacial cavities carved by meltwater erosion. Close resemblance of the Rogen

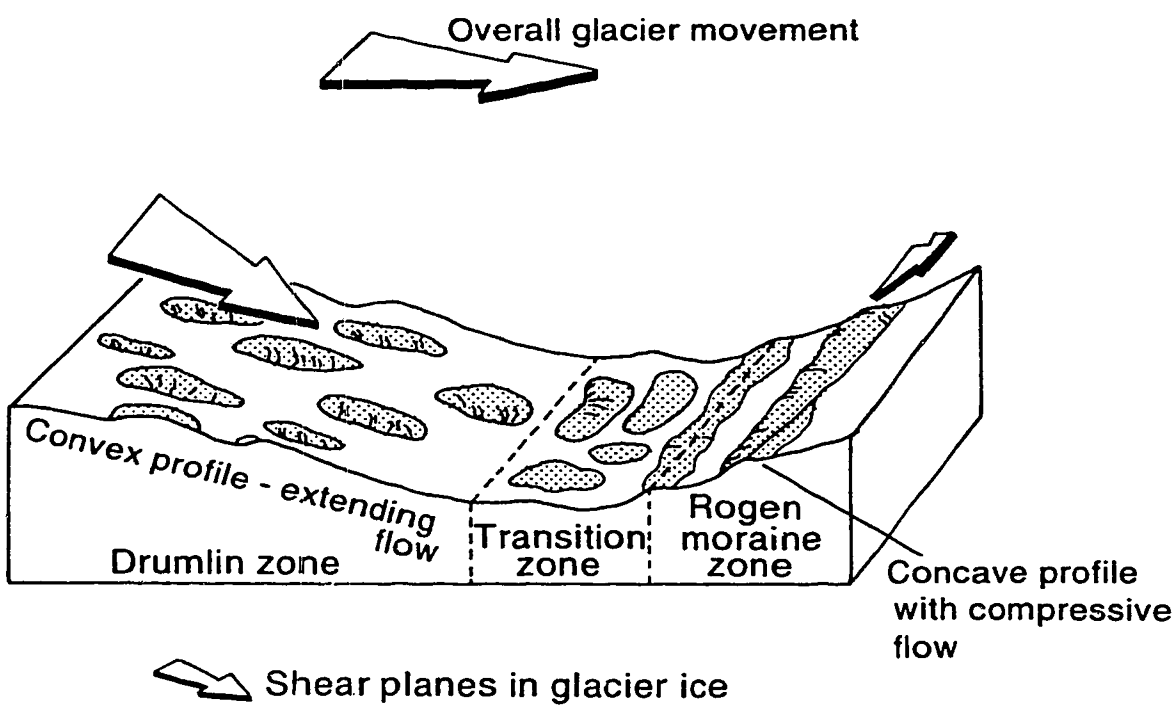

Figure 1. Zone of Rogen terrain formation in a topographic depression. After Sugden and John (1977).

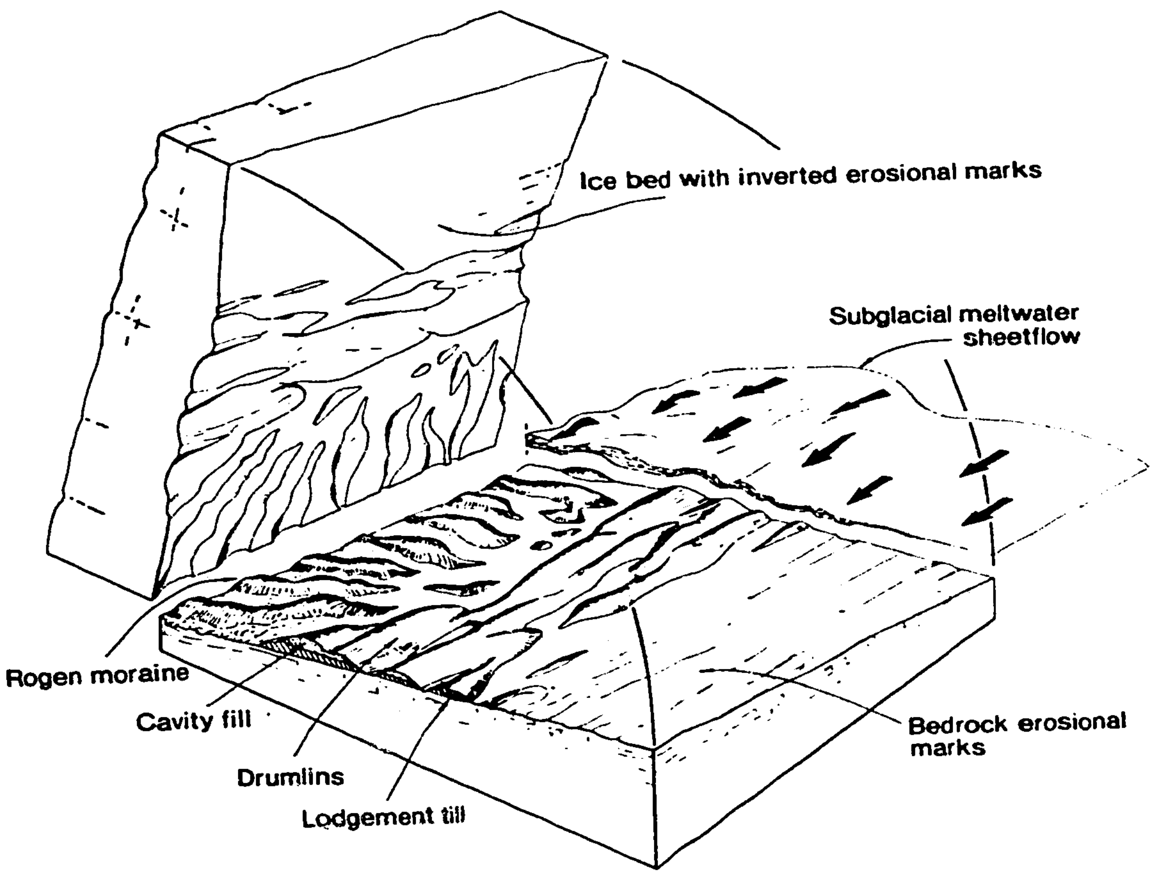

Figure 2. Formation of subglacial bed forms including the formation of Rogen terrain by infilling subglacial erosional cavities.
Source: Shaw (1988).

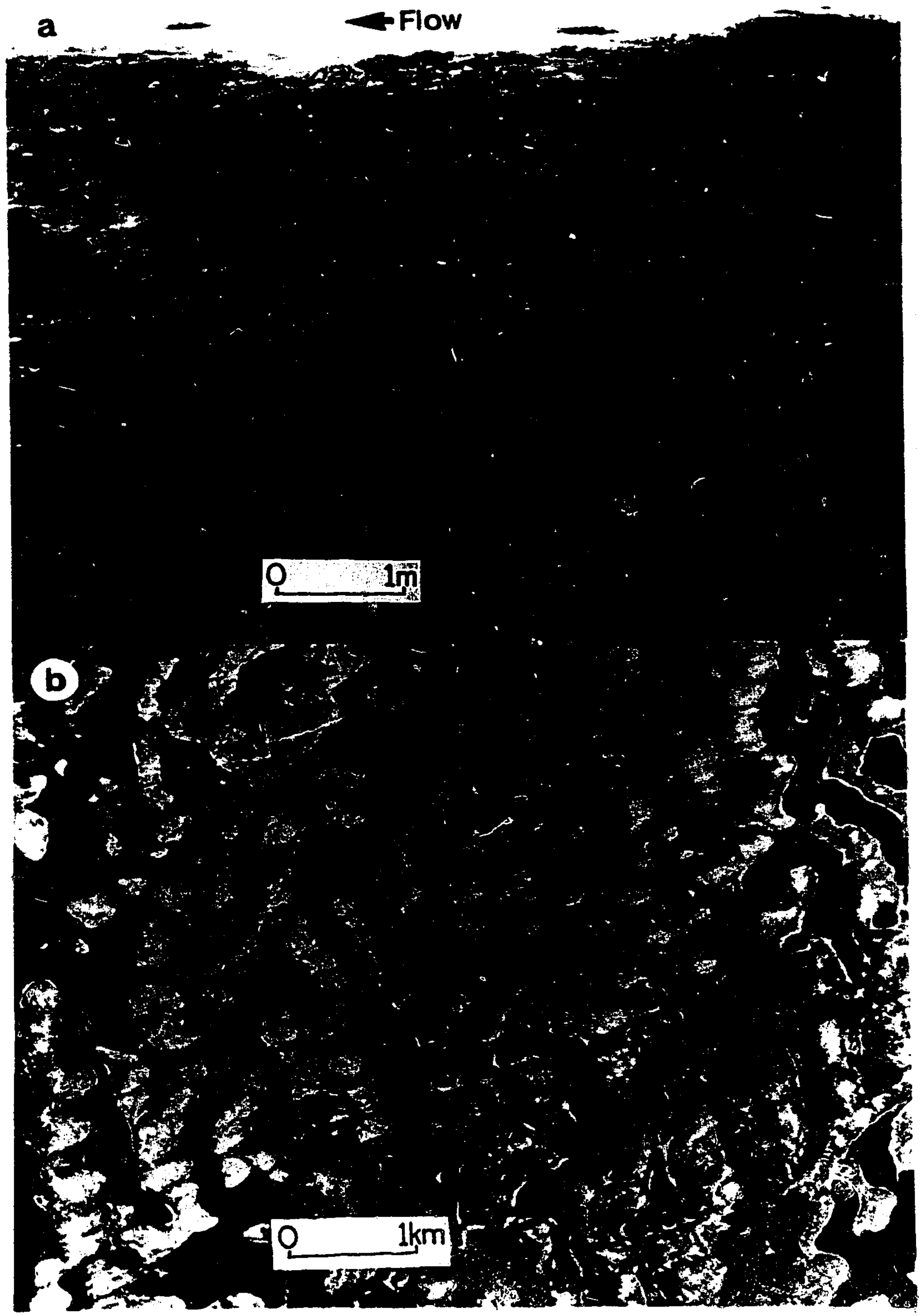

Plate 3. **a.** Erosional cavities carved in the underside of river ice.
b. Rogen moraine. North is to the top of photograph.
Source: Shaw (1988).

terrain ridges to erosional cavities carved in river ice (Plate 3) suggested that the Rogen terrain may represent debris-filled cavities which were first eroded by subglacial meltwater processes. The river ice and the Rogen terrain both display a convex form and bulbous knobs in the up-flow direction. A bifurcate structure typical of the ice pattern is also apparent in the Rogen terrain. Association of the Rogen terrain with drumlins has also provided evidence to suggest subglacial meltwater processes as being responsible for the formation of the Rogen terrain. As Lundqvist (1969) pointed out, the sequence of land forms ranging from Rogen terrain to drumlins represents a continuum of related features (Figure 3) formed under varying conditions. Shaw, Kvill, and Rains (1989) postulated that some drumlins are formed by subglacial meltwater processes. Since these features are generally found in elevated regions, it is possible that similar processes are responsible for the formation of Rogen terrain in topographic lows as part of the continuum suggested by Lundqvist. Based largely on the comparison of forms (from aerial photographic stereo pairs) and the relationship between Rogen terrain and drumlins, available evidence strongly supports a subglacial meltwater origin for Rogen terrain (Fisher and Shaw, 1992).

Hummocky Terrain

Hummocky terrain lacks the obvious consistent linear elements associated with Rogen terrain. This suggests that the dynamic conditions responsible for the development of Rogen terrain may not have formed hummocky terrain. Clayton and Moran (1974) proposed that, rather than systematic retreat, ice stagnated and down-wasted redistributing supra-glacial debris to form hummocks. There are a variety of hummocky type land forms which may represent this relief inversion process. However, the types examined in this study may represent more of an ice-pressed form (Hoppe, 1952; Stalker, 1960). Orientation of pebbles and compaction of the diamicton

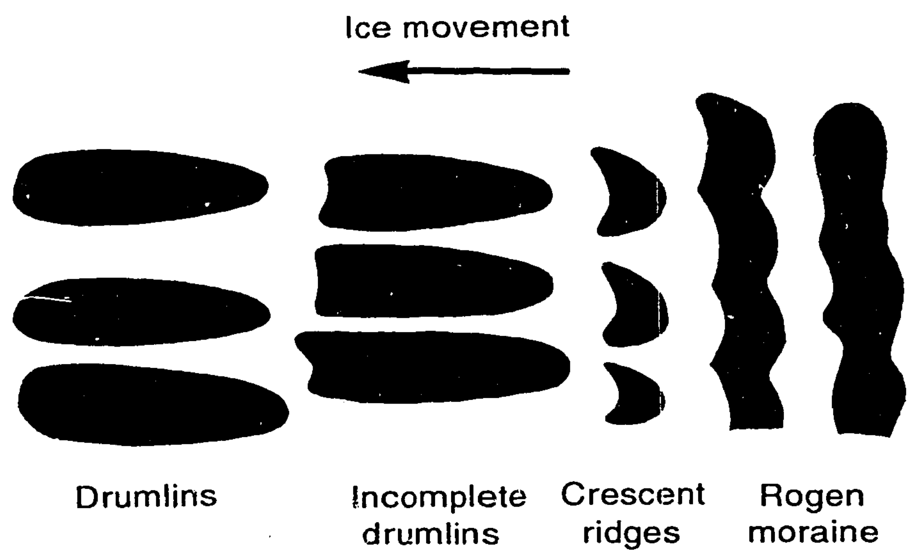

Figure 3. Transitional features related to varying depositional conditions. After Lundqvist (1969).

(poorly sorted, matrix-supported sediment) in the hummocks of Norrbotten, Sweden, provided the basis for the ice-pressed theory postulated by Hoppe (1952). He suggested that the disintegration of a dead-ice mass produces separate blocks which settle into a soft bed pushing the deformable material aside into the openings between the ice blocks, forming hummocks. This idea was supported by Stalker (1960) from his observations on the hummocky terrain of central Alberta. He went on to propose that the hummocks of this region may have been constructed during thickening of the ice sheet or lowering of the ice surface and they are "good indicators of conditions during deglaciation".

The regular patterns associated with the hummocky terrain are not easily explained by the ice-press theory of Hoppe and Stalker (Shaw, 1988). Nevertheless, Shaw (1988) produced a pattern similar to an inverted hummocky terrain landscape by subjecting a slab of plaster of Paris to direct erosion by low velocity water flow in a flume (Figure 4). The pattern produced on the plaster slab represents direct erosion of flowing water, identical to those occurring on the underside of an ice sheet. Upon settling of the ice sheet to the ground, a pattern similar to the hummocky terrain would then be produced in a deformable bed of material. Visual comparison between depressions of the plaster slab and the hummocky terrain suggest a fluvial origin for the hummocky terrain and a possibility that it was formed in a similar manner as the Rogen terrain (Shaw, 1988). This is a highly speculative analogy which receives some support in that hummocky terrain is closely associated with drumlins on the prairies of western Canada (Gravenor and Kupsch, 1959; Stalker, 1960, Clayton and Moran, 1974), and according to Lundqvist (1969) the transition from Rogen terrain to drumlins also represents a continuum. Thus hummocky terrain may have been formed by similar processes to those which formed Rogen terrain. However, there is a distinct

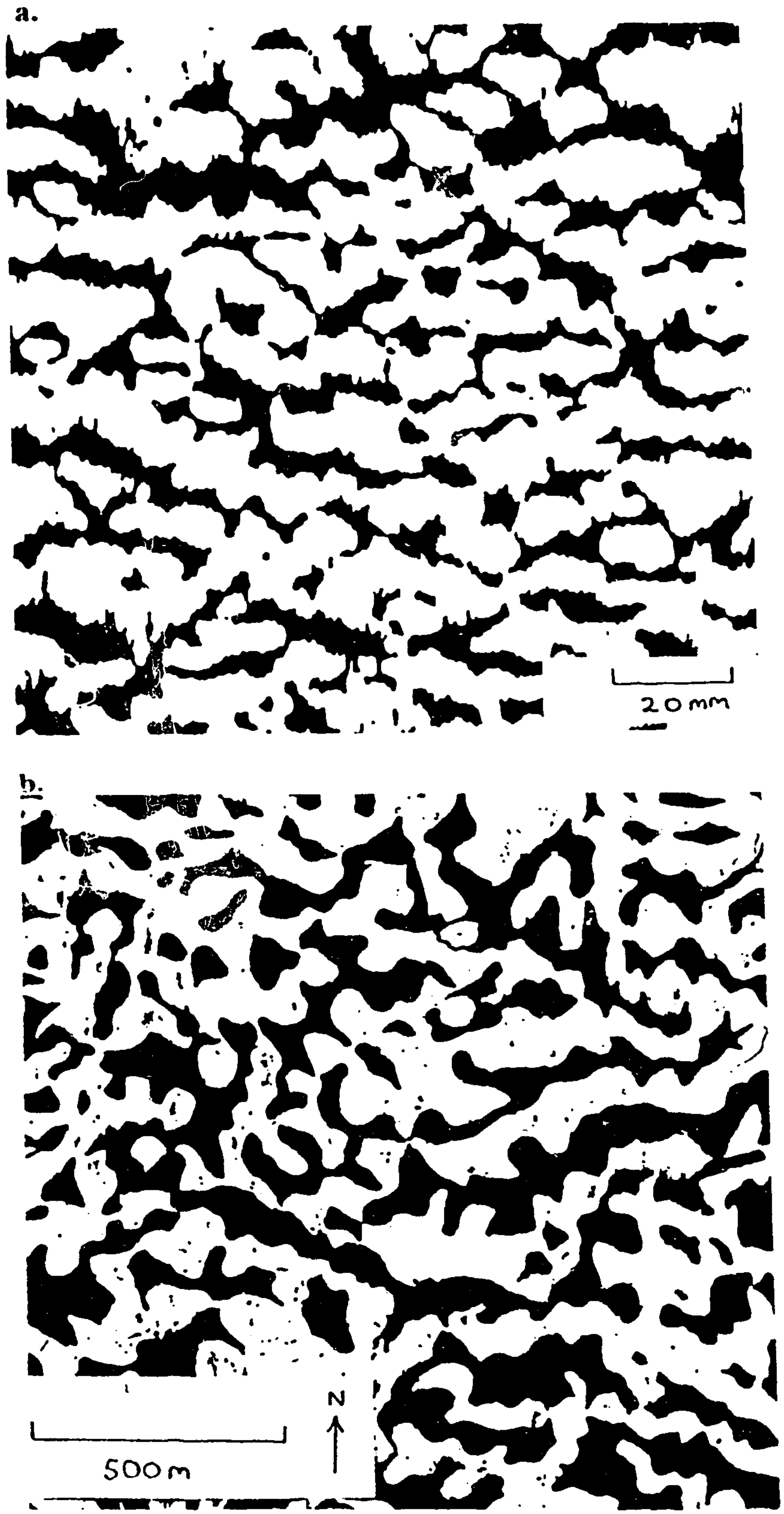

Figure 4. **a.** High contrast photograph of erosional pits in plaster of Paris.
b. Hummocky terrain in central Alberta. Dark areas are depressions shaded by hand from aerial photographic stereo pairs. Source: Shaw (1988).

difference, Rogen terrain is generally found in topographic depressions (Sugden and John, 1976) and hummocky terrain is usually on elevated ground (Stalker, 1960). Topographic differences may account for variations in meltwater flow conditions; deep, low velocity flows in landscape depressions may be related to the formation of Rogen terrain in these areas and shallow, higher velocity flows over the elevated areas may produce hummocks (Shaw, 1988). Although there is no direct sedimentary evidence available to support a fluvial origin for hummocky terrain in the Stettler area, comparison of forms (which have been largely overlooked by previous investigators) and the relationship between hummocky terrain and drumlins have provided additional evidence to explain the origin of this land form.

3. DATA BASE DEVELOPMENT

Subsequent to selecting the sample areas for form analysis, database development is in two main stages: **1.** interpretation and manual mapping, and **2.**digital data transformations. In the mapping stage, features to be used in the analyses were manually extracted from aerial photographs. Digital cartographic methods are then employed to transform the data into a usable format for analysis and display. Data collection and processing is performed using consistent methods wherever possible for all sample areas to retain integrity and comparability of specific physical features.

Study Sites and Sample Areas

Rogen terrain characterizes the first study site which is situated in the Northwest Territories, Canada (Figure 5). Drumlins and eskers associated with the Rogen terrain run roughly perpendicular to the long axes of the ridges of this "ribbed" landscape (Wright, 1967) indicating a ridge orientation transverse to the direction of the most recent glacial flow. Ridges range from approximately 500 m to 2000 m in length and 100 m to 300 m wide. Ridge crests stand 10 m to 30 m in height with a wavelength between crests averaging 300 m to 700 m. Lichen covered ridges are light in tone providing strong contrast between the dark water bodies and accentuating both the ridges and depressions.

A second study site, consisting of hummocky terrain, is located in central Alberta, Canada (Figure 5). This undulating topography consists of individual rolling hills, moraine plateaus, as well as elongated and connected ridges forming a complex, random pattern of mostly interconnected depressions. Individual hummocks average 3 m to 6 m in height with a base diameter varying from 40 m to 80 m. Moraine plateaus are the highest features of this landscape, reaching heights of up to 20 m. Continuous ridges throughout the hummocky terrain are highly variable in length ranging from 50 m to 1200 m long.

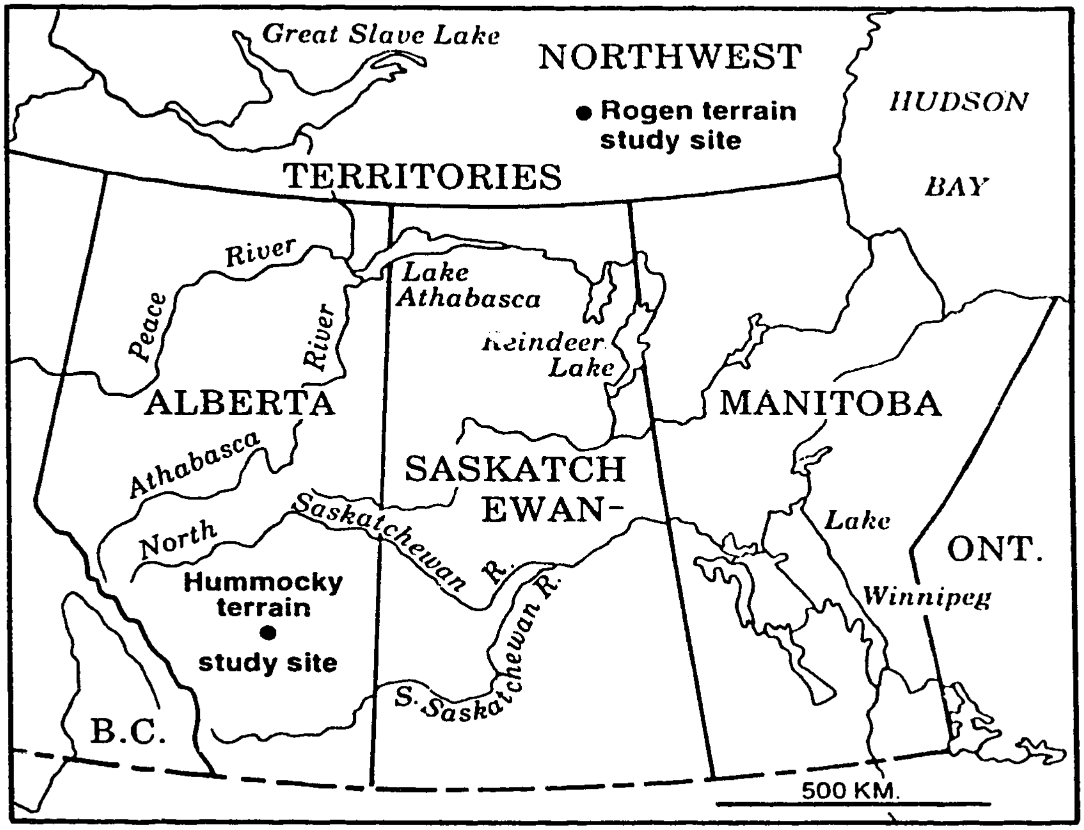

Figure 5. Rogen terrain and hummocky terrain study sites.

As indicated in chapter 1, the 'Rogen terrain' like landscapes found throughout hummocky terrain are more prominent in some areas than others, hence, three sample areas from the hummocky terrain were selected for analysis. The first two sample areas (H1 and H2) were selected as landscapes within the hummocky terrain which are qualitatively similar to those recognized in the Rogen terrain. The third sample area (H3) represents a landscape within the hummocky terrain where ridge and depressional features do not resemble the 'Rogen terrain' like pattern.

Absence of water bodies throughout most of the hummocky terrain make ridges and depressions less distinguishable than those of the Rogen terrain. However, stereo pair aerial photographs (Plates 4a and 4b) provide a three dimensional view of hummocky terrain showing ridge and depressional forms similar to the Rogen terrain. Being situated on the extreme western edge of the hummock field, the relief in Plate 4a (sample area H1) is much more subtle than that of Plate 4b (sample area H2), although the water-filled depressions in sample area H1 better accentuates the depressional forms. In both cases, ridge alignment and elongated depressions (similar to that of the Rogen terrain) are evident. Plate 4c (sample area H3) shows random undulating topography normally associated with hummocky terrain not conforming to the regular pattern characteristic of the Rogen terrain. A stereogram of the Rogen terrain was not included because the water bodies delineate higher and lower elevation terrain which accentuate the depressional form shapes more effectively than viewing the landscape under stereo paired aerial photographs (see Plate 1).

Mapping

Morphometric comparison of the Rogen terrain and the hummocky terrain requires that the features of interest be isolated from all unnecessary information. Ridges and depressional-form shapes were extracted from enlarged (3x) stereo pair aerial photographs with an original scale of 1:60,000 for the Rogen terrain and 1:15,000 for

a. Sample area H1.

b. Sample area H2.

c. Sample area H3.

Plate 4. Stereo pairs of sample areas H1, H2, and H3.

the hummocky terrain. A systematic approach to feature identification was employed to minimize subjective interpretation as information was transferred manually from the aerial photographs to Mylar film.

In the Rogen terrain, shapes were determined from water boundaries which provided distinct natural delineations between depressional areas and the higher elevation terrain. Shoreline boundaries were traced to define the depressions characteristic of the Rogen terrain. Throughout some areas of the hummocky terrain, shallow water bodies (sloughs) also provided the means for defining the shapes of depressional areas. For those areas within the hummocky terrain which lacked water bodies, depressions were identified as the inter-hummock regions bounded by sharp concave breaks in slope at the base of the hummocks. Despite the different methods for defining depressions, both measurements used distinct physical features to ensure a consistent extraction of depressional shapes from each land form image.

Water bodies, which defined the depressions areas in the Rogen terrain, were also effective in accentuating the higher elevation terrain (ridges). Continuous crests were recorded as ridges. Although the absence of water bodies throughout most of the hummocky terrain did not provide the contrast between depressions and elevated regions (as in the Rogen terrain), linear convex features were identified as ridges on the aerial photographic stereo pairs and recorded as lines on the Mylar overlay.

Digital Data Transformations

The analog information recorded on the Mylar film was digitized and converted to a vector format. All digitizing was performed in incremental mode which recorded digital points at equally spaced intervals along data lines. This technique was most efficient for digitizing convoluted shapes. Ridges were represented as a series of individual line segments of equal length. Formatted vector data files were then used to produce raster data files. Rasterized ridge and depressional shape files from corresponding sample areas were overlaid. Gray scale mapping techniques were then employed to produce binary images of ROG from the Rogen terrain study site (Figure 6) and binary images of the sample areas H1, H2, and H3 from the hummocky terrain study sites (Figures 7, 8, and 9). Ridges were represented as solid lines of one grid cell width and depressional shapes were displayed as filled polygons.

Figure 6. Binary image of depressional forms and ridge crests from sample area ROG.

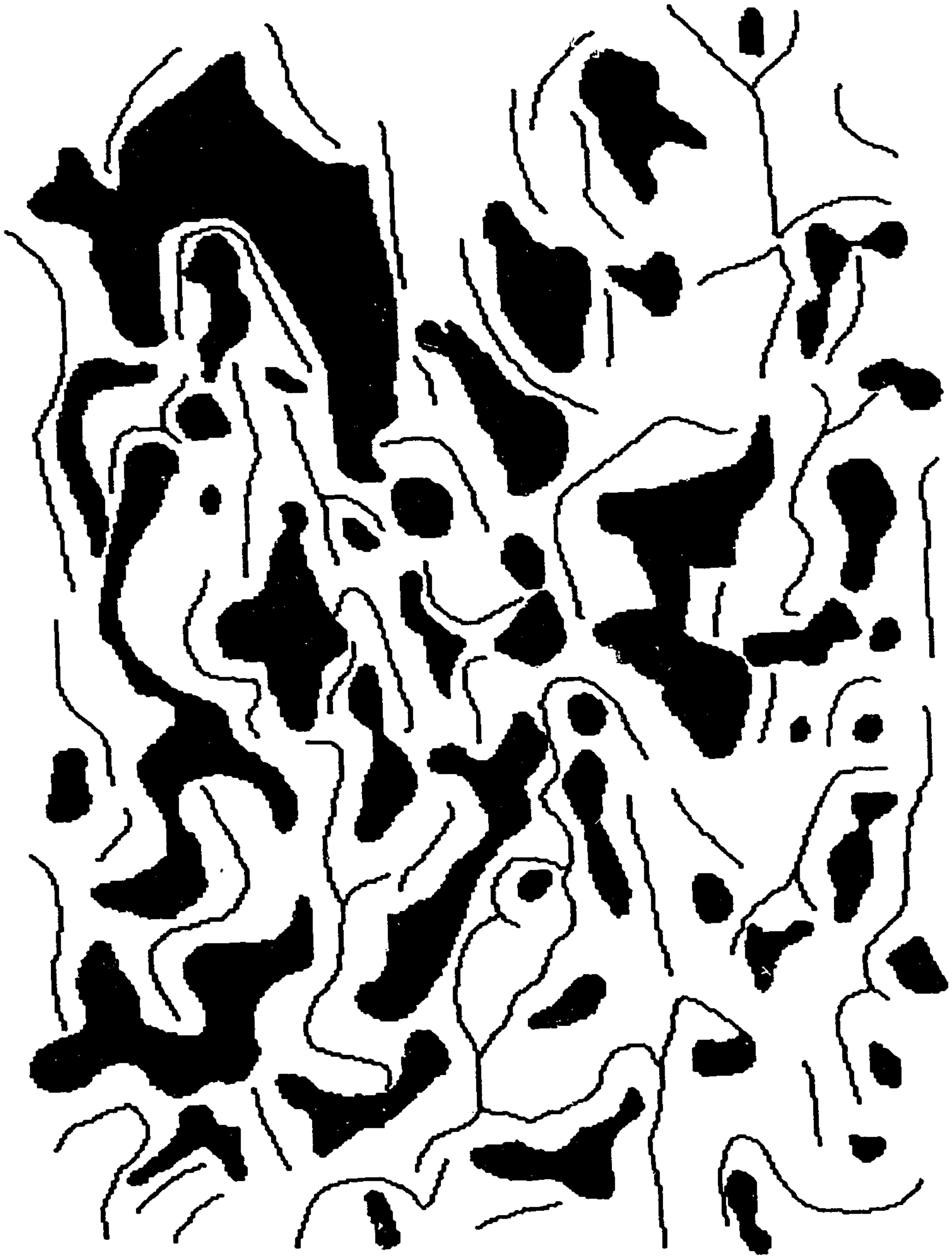

Figure 7. Binary image of depressional forms and ridge crests from sample area H1.

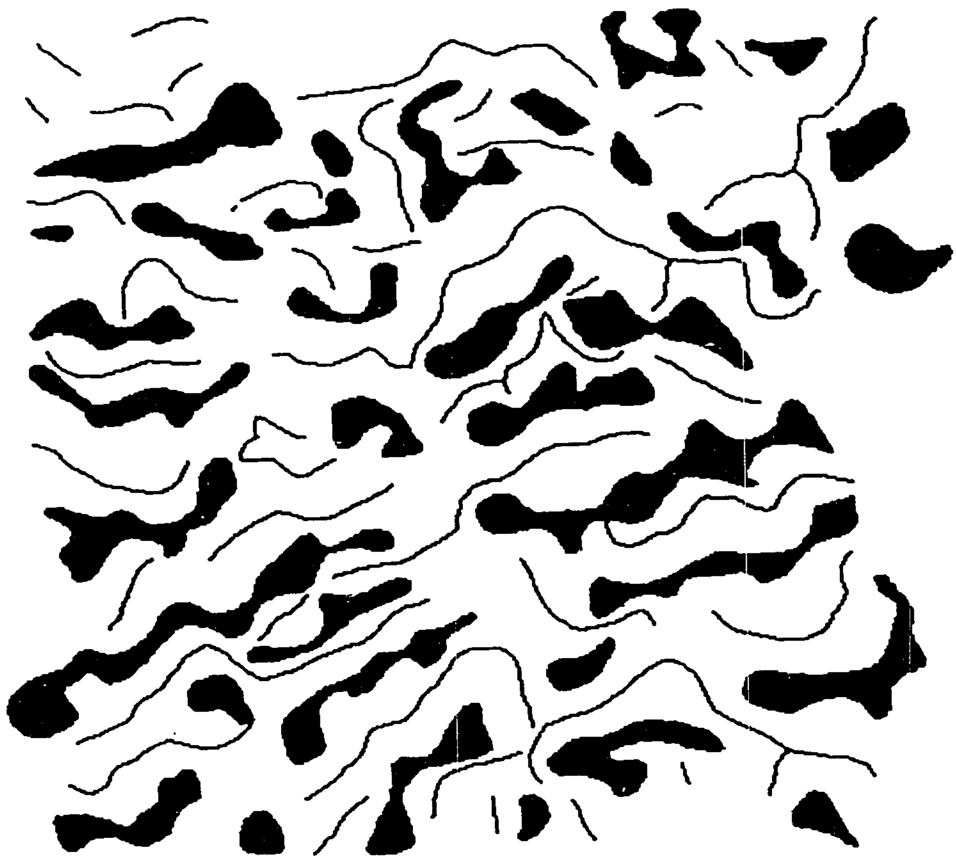

Figure 8. Binary image of depressional forms and ridge crests from sample area H2.

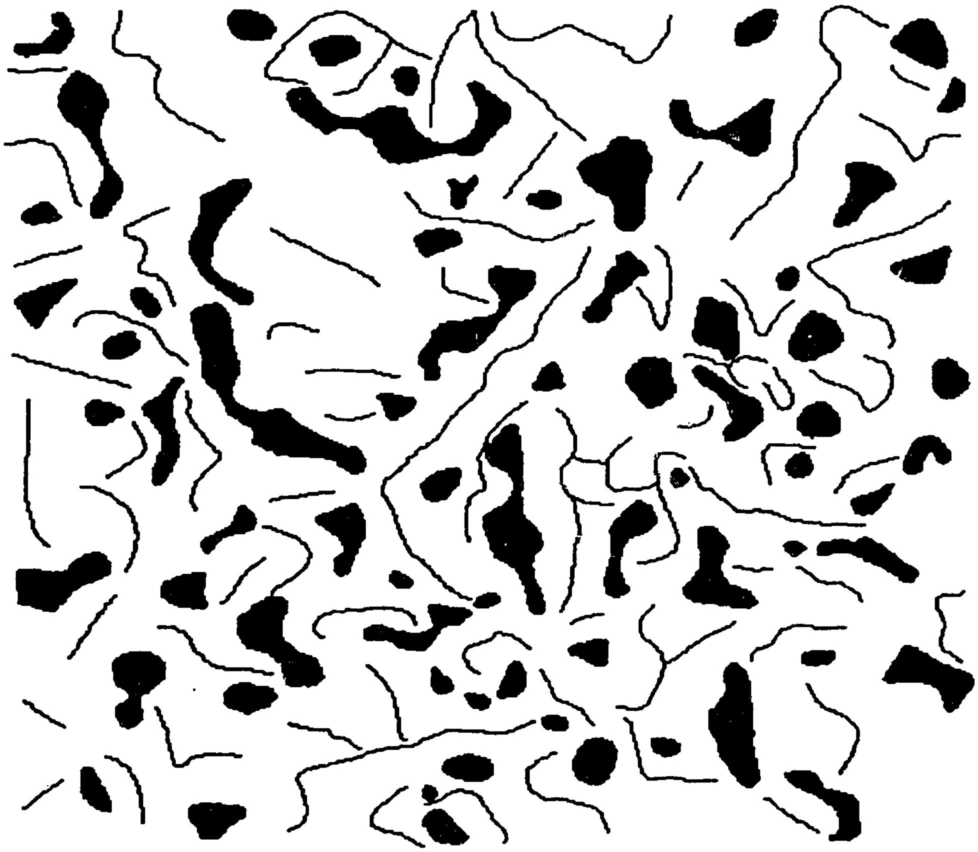

Figure 9. Binary image of depressional forms and ridge crests from sample area H3.

4. ANALYSIS OF SHAPE

Many techniques for measuring shape have been reported in the literature (Boyce and Clark, 1959; Lee and Sallee, 1970; Pavlidis, 1976; Clark, 1981) , but few techniques are capable of measuring the complex, highly contorted shapes such as those being examined in this study. A good review of shape measures as used in the earth sciences can be found in Davis (1986). In some instances different methods of shape analysis will provide different measures for the same shape (Lee and Sallee, 1970), therefore, this study employs four dimensionless shape analysis techniques (Pearson's Coefficient of Skewness, Compactness, Circularity, and Shape Factor) to provide an unbiased quantitative spatial measure of the depressional-form shapes. Statistical analyses were then performed to compare the terrain samples based on these four shape indices.

Shape Measurements

Pearson's Coefficient of Skewness (PCS) (Spiegel, 1961), was calculated from the distribution of distances between grid cells within each shape (Taylor, 1979). Pixels defining shapes were represented as '1' and background pixels were represented as '0'. Distances between each pixel and every other pixel within a particular shape were calculated and stored in an array. PCS values were then calculated from the distribution of distances using the expression given below:

$$PCS = (avg - med) / sd$$

where:

avg = average of distance measures
med = median of distance measures
sd = standard deviation of distance measures

Values for the other three shape indices were calculated from perimeter and area measures using the relationships shown below as provided by Folk (1968) and Moellering and Rayner (1979):

$$Circularity\ (CIR) = 4A / P^2$$

$$Compactness\ (COM) = P^2 / (4 * \pi * A)$$

$$Shape\ Factor\ (SF) = (P / Pc) * 100$$

where: A = area of shape
P = perimeter of shape
Pc = perimeter of a circle having the same area as the shape

Representative shapes selected from the Rogen terrain study site are shown in Figure 10 along with their corresponding shape indices. PCS is an indicator of elongation, puncturedness, and indentation. An increase in elongation results in an increase in this coefficient (see Figures 10a and 10d) whereas an increase in the degree of puncturedness or indentation corresponds to a decrease in this measure (see Figures 10b and 10c). CIR measures how close a shape approximates a circle (circularity). High values indicate a near circular form (see Figure 10b), while low values of this index indicate a convoluted or elongated shape (see Figures 10a, 10c, and 10d). COM measures shape indentation. Highly irregular shapes exhibited relatively low values while compact shapes with minimal indentation (see Figures 10b and 10d) produced relatively high values. SF also measures circularity and compactness, however this index is based solely on perimeter measures. Elongated and convoluted shapes (see Figures 10a and 10c) produced large SF indices while compact and near circular shapes (see Figures 10b and 10d) produced relatively small SF indices.

Statistical Testing

Table 1 shows the relationships (Pearson's product-moment coefficients of determination) between the shape indices for the depressional forms found in the Rogen terrain. Very similar results were obtained for relationships between the shape

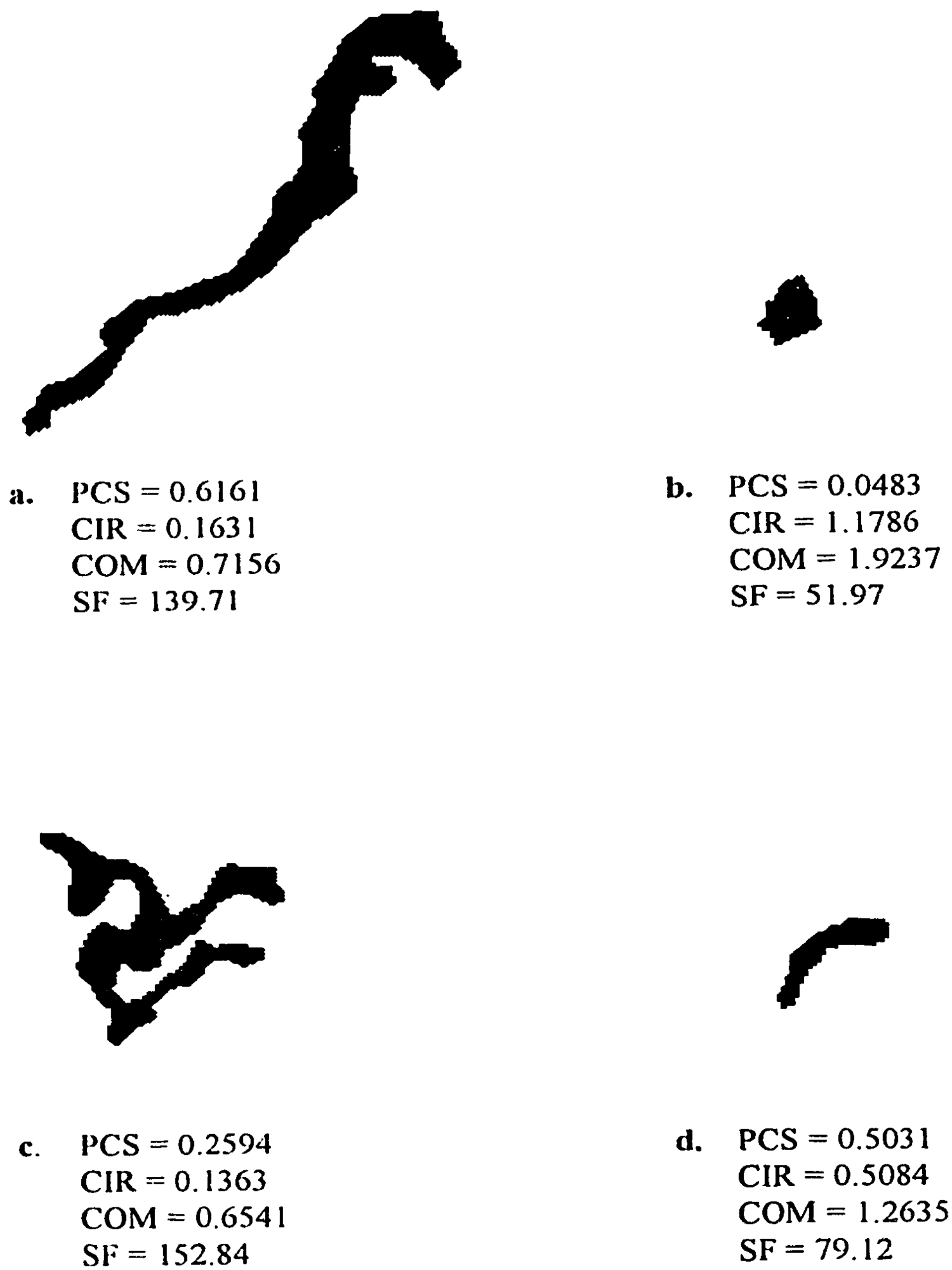

Figure 10. Representative shapes from Rogen terrain and corresponding shape indices.

Table 1. Coefficients of Determination for Shape Indices From Rogen Terrain

Shape Indices	Circularity	Compactness	Shape Factor	Skewness
Circularity	1.0000			
Compactness	0.9765	1.0000		
Shape Factor	0.7742	0.8842	1.0000	
Skewness	0.2367	0.1735	0.0525	1.0000

indices from the three samples of hummocky terrain. A high correlation between CIR, COM, and SF indicate a considerable amount of redundant information being conveyed by these indices. Conversely, PCS shows a low correlation with the other three shape indices. Due to the high correlation between perimeter and area based shape indices, and the independent nature of the skewness measure, the dominant properties of shape being measured here are compactness or circularity, and elongation.

Shape measurements of the depressional forms provided the basis for statistical comparisons between the hummocky terrain sample areas (H1, H2, and H3) and the Rogen terrain sample area (ROG). Table 2 shows the results of students *t* tests between sample areas based on difference of means testing. Test results were rejected or accepted at a 95% significance level; i.e. students *t* scores less than 1.96 indicated no significant difference between sample areas while students *t* scores of 1.96 or greater indicated sample areas were significantly different.

Students *t* scores between H1 and ROG for CIR, for COM, and for SF all indicate no difference between these sample areas. A larger students *t* score was noted between H1 and ROG for the PCS measure (compared to the other three shape indices), however there was still no significant difference between these samples. Students *t* scores for H2 and ROG indicated no difference between these sample areas for all shape indices. Sample areas H1 and H2 also exhibited no difference between them based on all shape indices of depressional forms. Shape measurements of depressional forms from H3 were unique among all other sample areas. Students *t* scores for all shape indices indicated no significant likelihood of H3 being similar to any other sample area.

Because students *t* tests were performed for each shape index, the probability associated with the differences between each sample area reflected similarities based on specific properties of shape. Strong similarities between H1 and ROG for CIR and

COM indices indicated that shapes from these sample areas are more similar based on closeness to circularity and indentation properties than the elongation properties associated with PCS index. H2 and ROG sample areas were more similar based on PCS and SF (elongation and perimeter measures) than on the properties associated with the CIR and COM shape indices.

Table 2. Students *t* Scores Between Sample Areas Based on Shape Indices

Test	Degrees of Freedom	PCS	CIR	COM	SF
H1 vs ROG	46	-1.67 (10.08*)	-0.26 (79.42*)	0.10 (91.82*)	-0.79 (43.20*)
H2 vs ROG	32	-0.61 (54.81*)	-1.25 (21.96*)	0.57 (29.51*)	0.57 (57.20*)
H3 vs ROG	57	-3.86 (0.03*)	3.20 (0.21*)	-3.56 (0.16*)	-3.56 (0.01*)
H1 vs H2	32	-1.10 (27.85*)	1.44 (16.06*)	1.47 (15.21*)	-1.33 (19.41*)
H1 vs H3	46	1.96 (5.6*)	-3.49 (0.11*)	-3.49 (0.25*)	3.02 (0.42*)
H2 vs H3	32	2.24 (3.21*)	-5.35 (0.01*)	5.29 (0.00*)	5.29 (0.00*)

*Probability of "no difference" between sample means (%).

5. RIDGE ORIENTATION ANALYSIS

Ridges from each sample area were analyzed to determine whether or not the pattern of orientations indicate a specific trend. Visual inspection of the Rogen terrain indicates that the ridges of this land form type exhibit a preferred trend; a significant alignment of ridges throughout the hummocky terrain may be an additional indicator that the Rogen terrain and the hummocky terrain share the same genesis.

The ridges were digitized as a series of line segments whose end points were defined by X and Y Cartesian coordinates. The length of each individual line segment was not used as part of any calculations, consequently all line segments were of the same length to maintain equal proportions of directional measure. For example, long straight sections were represented by many line segments measuring a specific direction while shorter sections were represented by fewer line segments, thus contributing a fewer number of directed segments to that particular orientation. Line segments were digitized at sufficient resolution to measure maximum directional variance of each ridge. This was achieved by placing the X-Y coordinates at points of inflection along all ridges from each sample area. Half the length of the shortest distance between two data points was then used as the segment length to ensure that segment resolution was sufficient to measure all significant changes in ridge direction.

Line segments have two directions, a calculated direction, and an associated diametrically opposed direction. Krumbein (1939) proposed a simple method for transforming directional data into orientation data by "doubling" all measured angles resulting in a common set of orientations. For example, if two angles (of opposing direction but identical orientation), 60 degrees and 240 degrees were doubled, the resulting orientation angles would become the same. Doubling 60 degrees equals 120 degrees, and doubling 240 degrees equals 480 degrees, which also becomes 120 degrees (480 degrees - 360 degrees = 120 degrees) when plotted on a 360 degree circle (Davis, 1986).

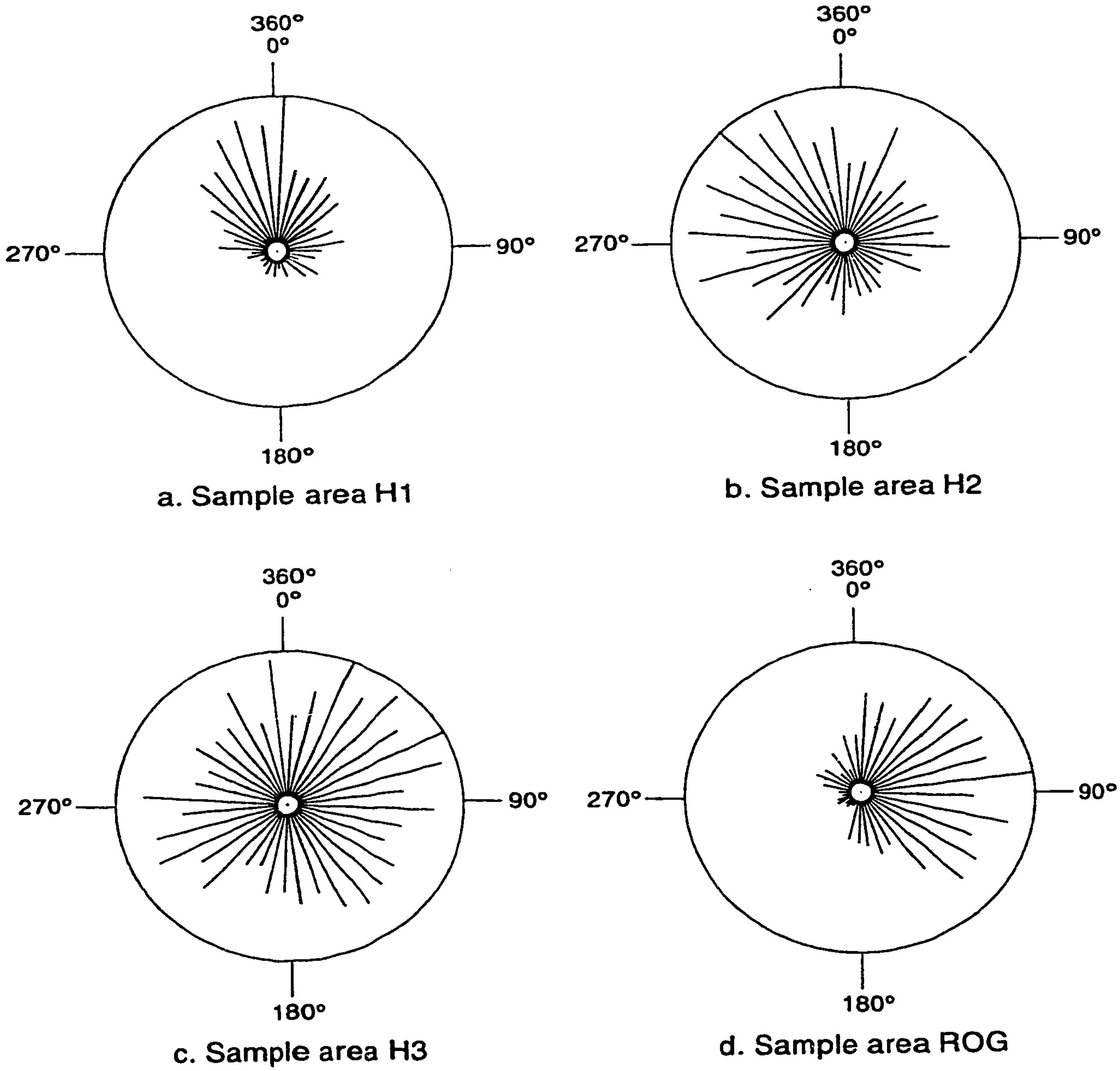

Figure 11. Ridge orientations from sample areas after transformation.

Figure 11 displays the angles from each sample area plotted as a polar graph after the transformation to orientations. The circular distribution was divided into 36 classes using a 10 degree class interval. Each class was represented by a single vector whose length was determined by the number of angles contained in that particular class. Visual inspection of the plots show that sample areas H1 and ROG (Figures 11a and 11d have preferred trends. Sample area H2 (Figure 11b) has slightly greater dispersion than H1 and ROG, and sample area H3 (Figure 11c) appears random.

Concentration values for each dispersal pattern were calculated by computing the resultant vector for each sample distribution (all vector calculations are after Davis, 1986) . The resultant vector is a measure of dispersion of the circular distribution which ranges in value from 0.0 to 1.0; values near 0.0 represent a widely dispersed or uniform distribution and values close to 1.0 indicate that the distribution is highly concentrated. The resultant vector is dependent not only on the dispersion in the sample distribution, but also on the number of vectors being analyzed. Components of the resultant vectors must first be standardized in order to compare distributions obtained from different sample sizes. This is achieved by simply dividing each component of the resultant vector by the total number of sample observations. Calculation of the vector components of the standardized resultant vector are shown below.

$$\overline{C} = 1/n \sum_{i=1}^{n} \cos \theta i$$

$$\overline{S} = 1/n \sum_{i=1}^{n} \sin \theta i$$

where: n = number of observations
θ = orientation in degrees

The resultant vector for each distribution was then calculated from the Pythagorean theorem.

$$\bar{R} = \sqrt{\bar{C}^2 + \bar{S}^2}$$

The concentration of each sample distribution is indicated by the magnitude of the resultant vector (Table 3).

Samples were then statistically tested to determine whether or not the ridge orientations from each sample are representative of samples selected from populations of uniform distribution. The test for randomness (for large values of *n*) is given by Stephens (1969). The null hypothesis *Ho* states that the sample belongs to a population of uniform distribution. The test was calculated at a 95% confidence level as follows.

If $R^2 > -2n \ln \alpha$,

where: n = number of observations
$R = \bar{R}n$
α = significance level,

then reject *Ho*, concluding that the sample has a preferred orientation.

Table 4 shows the results of testing for a preferred orientation from all sample areas. For sample areas H1, H2, and ROG, the null hypothesis is rejected at a 95% confidence level indicating that ridge orientations from these sample areas were drawn from populations having a preferred orientation. The null hypothesis for sample area H3 is accepted at a 95% confidence level indicating that this sample area was drawn from a population having random ridge orientations.

Table 3. Resultant Vectors for Ridge Orientations From Sample Areas H1, H2, H3, and ROG

Sample Area	Number of Observations	Resultant Vector (R)
H1	1256	0.4267
H2	864	0.2119
H3	1002	0.0738
ROG	1065	0.4092

Table 4. Results of Testing For a Preferred Orientation From Sample Areas H1, H2, H3, and ROG.

Sample Area	R^2	$-2n \ln \alpha$	*Ho**
H1	287227	7525	reject
H2	33519	5177	reject
H3	5468	6003	accept
ROG	287227	6381	reject

**Ho*: sample was drawn from a population of uniform distribution.

$\alpha = 0.05$ (95% confidence level)

6. CONCLUSIONS

Analytical cartographic techniques have provided quantitative evidence to support a genetic relationship between the hummocky terrain of central Alberta and the Rogen terrain of the Northwest Territories. Depressional form shapes and ridge orientation patterns are significantly similar between sample areas H1 and H2 from the hummocky terrain study site and sample area ROG from the Rogen terrain study site. Statistical comparison of the same properties between sample areas H3 and ROG revealed significant differences indicating that the regular pattern associated with the Rogen terrain does not persist throughout the entire hummocky terrain landscape.

Analysis of depressional forms and ridge orientations were used to provide a comparison based on the dominant areal and linear properties common to both the hummocky terrain and the Rogen terrain landscapes. Form measurement comparisons included four separate shape index values which examined various characteristics of each shape. Significant similarity between sample areas H1, H2, and ROG based on all shape index values indicated that the shapes of these sample areas are essentially identical. Orientation analysis was used to determine the strength of concentration of ridge alignment. A preferred trend in sample areas H1, H2, and ROG indicated a regular geomorphic pattern associated with these sample areas, while uniform ridge orientations in sample area H3 indicated a random pattern associated with this sample area. Morphometric comparisons of the Rogen and hummocky terrain land forms were based on two disparate measures (areal shapes and linear trends) to ensure valid conclusions.

The results of this study suggest that at least two general land form patterns exist throughout the hummocky terrain; sample areas H1 and H2 which are both significantly similar to sample area ROG, and sample area H3 which is significantly different from sample area ROG. The presence of at least two distinct land form patterns characteristic of the hummocky terrain suggests that the process responsible for the formation of the hummocky terrain was operating under variable conditions. The 'Rogen terrain' like characteristics of sample areas H1 and H2 suggest that the processes of formation may have been similar between these particular areas of the hummocky terrain study site and the Rogen terrain study site. Sample area H3 which does not exhibit the 'Rogen terrain' like characteristics was likely formed by the same process that developed the rest of the hummocky terrain, but under different conditions.

The main conclusion of this study supports a similar process of formation for the Rogen terrain as for the hummocky terrain. This implies that the hypothesis proposed by Shaw (1988), to explain the origin of the Rogen terrain by subglacial meltwater sheet flow (as discussed in chapter 2), may also be applicable to the hummocky terrain. However, this study was solely concerned with the relationship in form between the Rogen and the hummocky terrain landscapes, and does not invoke a particular process for the formation of either land form.

Digital cartographic techniques and statistical analysis have shown that significant similarities exist between sample areas H1, H2, and ROG. These similarities suggest that a relationship may exist between the hummocky terrain and the Rogen terrain and thus provides evidence to support similar process of formation for both features. The hummocky terrain of central Alberta and the Rogen terrain of the Northwest Territories appear to have a common or similar origin.

REFERENCES

Boyce, R. R., and Clark, W.A.V. 1959. The concept of shape in geography. Geographical Review, pp. 61-573.

Clark, M.W. 1981. Quantitative shape analysis: a review. Mathematical Geology, **13**, pp. 303-319.

Clayton, L., and Moran, S.R. 1974. A glacial process-form model. In Coates, D.R., Glacial Geomorphology, Publications in Geomorphology, Binghampton, State University of New York, pp. 89-119.

Cowan, W.R. 1968. Ribbed moraine: till fabric analysis and origin. Canadian Journal of Earth Sciences, **5**, pp.1145-1159.

Davis, J.C. 1986. Statistics and data analysis in geology. John Wiley and Sons inc., 2nd Ed., London, p. 646.

Fisher, J.G., and Shaw, J. 1992. A depositional model for Rogen moraine, with examples from the Avalon Peninsula, Newfoundland. Canadian Journal of Earth Sciences, **29**, pp. 669-686.

Folk, R.L. 1968. Petrology of sedimentary rocks. Hemphill's, Austin Texas, p. 184.

Gravenor, CP., and Kupsch, W.O. 1959. Ice disintegration features in western Canada. Journal of Geology, **67**, pp. 48-64.

Henderson, E.P. 1959. A glacial study of central Quebec-Labrador. Geological Survey of Canada, Bulletin 50.

Hoppe, G., 1952. Hummocky moraine regions with special reference to the interior of Norbotten. Geographiska Annaler, **34**, pp.1-71.

Hughes, O.L. 1964. Surficial Geology, Nichicun-Kaniapiskau map area Quebec. Geological Survey of Canada, Bulletin 10G.

Ives, J.D. 1956. Till patterns in central Labrador, Canadian Geographer, No.8, pp. 25-33.

King, C.A.M. 1974. Morphometry in glacial geomorphology. In Coates, D.R., ed., Glacial Geomorphology, Publications in Geomorphology, State University of New York, Binghampton, pp. 147-162.

Krumbein, W.C. 1939. Preferred orientation of pebbles in sedimentary deposits. Journal of Geology, **47**, pp. 673-706.

Lee, D.R. and Sallee G.T. 1970. A method of measuring shape. Geographical Review, **60**, pp. 555-563.

Lundqvist, J. 1969. Problems of the so-called Rogen moraine. Sveriges geol. Unders. (c) 648, pp. 1-32.

Moellering, H. and Rayner, J.N. 1979. Measurement of shape in geography and cartography. Ohio State Univ., Report of the Numerical Cartography Laboratory, NSF Grant No. SOC77-11318, p. 109.

Pavlidis, P. 1978. A review of algorithms for shape analysis. Computer Graphics and Image Processing, **7**, pp. 243-258.

Shaw, J., and Ashley, G. 1988. Glacial facies models - Continental terrestrial environments. Geological Society of America, p. 121.

Shaw, J., Kvill, D., and Rains, B. 1989. Drumlins and catastrophic subglacial floods. Sedimentary Geology, **62**, pp. 177-202.

Spiegel, M. R. Theory and problems of statistics. 1961.

Stalker, A. Mac S. 1960b. Ice-pressed drift forms and associated deposits in Alberta. Geological Survey of Canada Bulletin 37, p. 38.

Stephens, M.A. 1969. Tests for randomness of direction against two circular alternatives. American Statistical Association Journal, **64**, pp. 280-289.

Sugden, D.E., and John, B.S. 1977. Glaciers and landscape - a geomorphological approach. Edward Arnold, London, p. 369.

Taylor, P.J. 1971. Distances within shapes: an introduction to a family of finite frequency distributions. Geografiska Annaler, **53B**, pp. 40-53.

Wright, G.M., 1967. Geological notes on the central district of Keewatin, Northwest Territories. Geological Survey of Canada, pp. 55-77.